J. Meas. Sci. Instrum., 2024, 15(1): 1-8.
DOI: 10.62756/jmsi.1674-8042.2024001
http://jmsi.publish.founderss.cn/
jmsi@nuc.edu.cn

Indirect measurement method for digging force of hydraulic excavator

SUN Tianyu*, ZHANG Ping, ZHANG Sen, TONG Kunhong
School of Mechanical and Electrical Engineering, Xi'an University of Architecture and Technology, Xi'an 710055, China

***Corresponding author:** SUN Tianyu (stysunshine@163.com)

Received: February 11, 2023 **Revised:** April 16, 2023 **Accepted:** April 23, 2023

Abstract: The digging force of hydraulic excavator is an important parameter reflecting the working conditions of the excavator. In this study, by analysis of the working mechanism of the excavator, a mathematical model reflecting the relationship between the cross-section stress of the linkage mechanism and the digging force of the bucket was established, and a new method for measuring the digging force was proposed. Furthermore, the cross-section stress values of the linkage mechanism under different digging forces were obtained by finite element simulation, and the error between simulation results and theoretical results was about 8%, which verifies the feasibility of the proposed measurement method for the digging force of hydraulic excavator.

Key words: hydraulic excavator; stress mesurement; digging force; finite element simulation

0 Introduction

In recent years, with the development of intelligent technology and driverless technology, excavators can gradually work in special environments such as high temperature and large mining areas, as well as the environments with radioactive materials and poisonous gases[1]. However, when an excavator is working in a high-complexity environment, its stability may be greatly reduced. To ensure the working stability of an excavator, its working condition must be monitored[2]. Currently, the intelligent driverless excavators have made great progress and been applied in pressure monitoring of hydraulic system, displacement monitoring of cylinder piston, image processing[3-5], etc. However, there is no more effective online measurement method for digging force.

The digging force is not only an important basis for the structural design and strength calculation of the working device, but also an important parameter reflecting the working conditions of the excavator. In the working process, it is often impossible to get accurate real-time digging force magnitude, which leads to the inability of the equipment to adjust the working parameters and operating conditions according to the changes in the environment[6]. Similarly, the digging force is an important parameter for evaluating the performance of excavators. Therefore, many scholars have carried out research on the calculation and measurement method of the digging force. Flores et al.[7] calculated the maximum digging force of the front shovel excavator based on the kinematic converter using linear optimization. It is actually a calculation of theoretical maximum digging force of working device. Bai et al.[8] conducted a joint simulation using Pro/E and ADAMS software. After a virtual prototype with XCG60-8A hydraulic excavator as a reference was built, the simulation analysis and digging force measurement of the model were carried out in the virtual environment. This method solves the maximum digging force of a hydraulic excavator under specific working conditions. However, because the prototype model ignores too many secondary factors, the measureed digging force has a large error. Jiang et al.[9] and Yu et al.[10] used pin sensors to measure digging resistance indirectly. This method needs to redesign the structure of arm joint and hinge pin. In addition, the measuring result is affected by the hinge gap and friction[11].

In our work, an indirect measurement method for digging force was proposed by means of the cross-section stress measurement of the connecting rod based on an established mathematical model feflecting the relationship between the cross-section stress of the linkage mechanism and the digging force of the bucket. This method can realize the effective measurement of the digging force without redesigning the structure of the

component owing to short force transmission path.

1 Mechanical analysis of working device of hydraulic excavator

1.1 Establishment of global coordinate system for working device

The working device of excavator is the key mechanism of excavator movement[12]. The mechanical analysis of the excavator's working device is not only the basis for studying the mathematical relationship between the hinge points of the excavator's working device and the components, but also the basis for establishing the "connecting rod stress-digging force" measurement model. A global coordinate system is established, as shown in Fig.1, with the location of the excavator as X-axis, and the right direction as positive; Y-axis passing the excavator's slewing center and perpendicular to the X-axis , upward direction as positive. Each hinge point is represented by capital letters, and the coordinates of each point are represented by a subscript symbol.

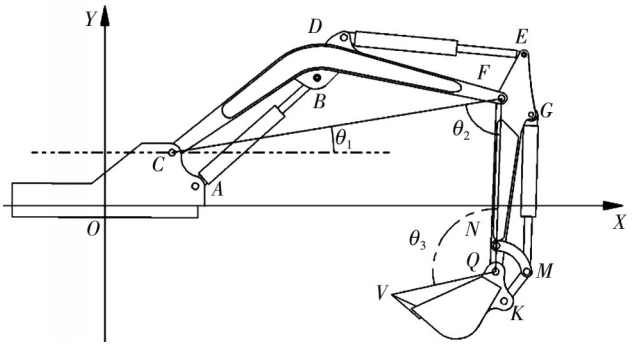

Fig. 1 Global coordinate system of working device of a hydraulic excavator

The position of excavator working device is mainly determined by boom angle θ_1, stick angle θ_2 and bucket angle θ_3. In the following section, the kinematic relationship between boom, bucket arm and bucket link will be analyzed..

1.2 Analysis of kinematic relationship between components

The rotation angle of the boom can be obtained by the cosine theorem as

$$\angle ACB = \arccos\left(\frac{l_{12}^2 + l_2^2 - l_{AB}^2}{2l_{12}l_2}\right), \tag{1}$$

$$\angle BCU = \angle ACB - \alpha_1, \tag{2}$$

$$\theta_1 = \angle BCU - \angle BCF, \tag{3}$$

where l_{AB} is the distance between joint point A and joint point B; l_{12} is the distance between joint point C and joint point B; l_2 is the distance between joint point C and joint point A; α_1 is the angle between the horizontal line and the connecting line of joint point C and joint point F; $\angle BCF$ is the angle between the connecting line CB and the connecting line CF; and $\angle BCU$ is the angle between the connecting line CB and the horizontal line.

In the global coordinate system, $\angle DFE$ can be obtained by the cosine theorem as

$$\angle DFE = \arccos\left(\frac{l_5^2 + l_7^2 - l_4^2}{2l_5l_7}\right), \tag{4}$$

$$\theta_2 = 2\pi - \angle DFC - \angle EFG - \angle DFE - \angle GFN - \angle NFQ, \tag{5}$$

where l_4 is the distance between joint point D and joint point E; l_5 is the distance between joint point D and joint point F; and l_7 is the distance between joint point E and joint point F.

As for the bucket and linkage mechanism of an excavator, it can be obtained from the cosine theorem as

$$\angle GNM = \arccos\left(\frac{l_{GN}^2 + l_{NM}^2 - l_{GM}^2}{2l_{GN}l_{NM}}\right), \tag{6}$$

$$\angle MNQ = \angle GNQ - \angle GNM, \tag{7}$$

$$\theta_3 = 2\pi - \angle FQN - \angle MQN - \angle KQM - \angle KQV, \tag{8}$$

where l_{GN} is the distance between joint point G and joint point N; l_{NM} is the distance between joint point N and joint point M; and l_{GM} is the distance between joint point G and joint point M.

By analysis of the above geometric relationship, boom angle θ_1, stick angle θ_2, bucket angle θ_3 as well as the angle relationship between the components can be obtained. Similarly, the coordinates of hinge point C at the bottom of the boom are also fixed and known in the global coordinate system of the working device. In summary, the coordinates of key hinge points $N(N_X, N_Y)$, $M(M_X, M_Y)$, $K(K_X, K_Y)$ and $Q(Q_X, Q_Y)$ of the linkage mechanism in the global coordinate system can be obtained.

2 Mechanical analysis of bucket and linkage mechanism

In the actual working conditons, the external load on the tooth tip of an excavator is changeable and complex, so it is very complicated and inconvenient to analyze the force on the working device alone. Therefore, the main load is retained in the analysis process, and the unimportant factors are simplified[13]. The simplified content is as follows.

1) The error caused by local design size is ignored.

2) The wear and friction at the joints of components are ignored.

3) Because the dead weight of the hydraulic cylinder is far lower than the digging force produced by the bucket, the hydraulic cylinder is treated as a two-force rod.

4) The energy transfer of bars and connecting parts is complicated and difficult to calculate. Therefore, according to the ideal conditons, the separated bucket-connecting rod part is regarded as a rigid structure, and the energy transfer loss between components is ignored.

5) The load on tooth tip only considers horizontal load while does not discuss the lateral load and eccentric load.

6) The dead weight of the bucket is considered.

According to the above assumptions, the mechanical analysis of the simplified model of bucket and linkage mechanism was carried out [14], as shown in Fig. 2. The X-axis passing through hinge point Q and parallel to the working ground of the excavator is taken as the positive side of the bucket; The Y-axis passes through cross joint point Q and is perpendicular to the X-axis, with the vertical upward direction as the positive direction. Thus, a local coordinate system is established.

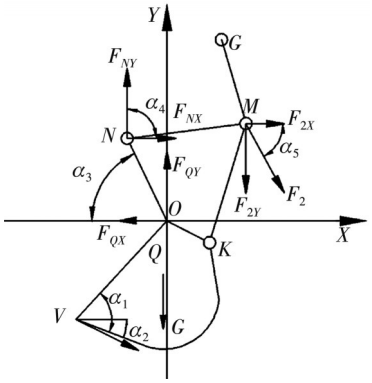

Fig. 2 Force analysis of bucket and linkage mechanism

The torque equilibrium equation of the bucket and the linkage mechanism is established as

$$l_{QV}F_V\sin\alpha_1+l_{GQX}G=l_{QMY}F_{2X}+l_{QMX}F_{2Y}+l_{QNX}F_{NY}+l_{QNY}F_{NX}, \tag{9}$$

where F_V represents the tangential non-offset external load on the tip of the bucket; G is expressed as the gravity of the bucket. In addition, we have

$$l_{QMY}=M_Y-Q_Y, \tag{10}$$

$$l_{QMX}=M_X-Q_X, \tag{11}$$

$$l_{QNX}=Q_X-N_X, \tag{12}$$

$$l_{QNY}=N_Y-Q_Y, \tag{13}$$

$$l_{GQX}=Q_X-G_X, \tag{14}$$

where l_{QMY} is the vertical distance between joint point M and joint point Q; l_{QMX} is the horizontal distance between joint point M and joint point Q; l_{QNX} is the horizontal distance between joint point N and joint point Q; l_{QNY} is the vertical distance between joint point N and joint point Q; l_{GQX} is the vertical distance between the bucket gravity and joint point Q; and l_{QV} is the distance between joint point Q and tooth tip V.

The force balancing equation is established with bucket and linkage mechanism as a whole, that is

$$F_{QX}-F_{NX}-F_{2X}-F_V\cos\alpha_2=0, \tag{15}$$

$$F_{QY}-F_{NY}-F_{2Y}-G-F_V\sin\alpha_2=0, \tag{16}$$

where F_{2X} is the force component of F_2 in the X-axis direction; F_{2Y} is the force component of F_2 in the Y-axis direction; F_{QX} is the component of force in the X-axis direction at joint point Q; F_{QY} is the component of force in the Y-axis direction at joint point Q; F_{NX} is the component of force in the X-axis direction at joint point N; F_{NY} is the component of force in the Y-axis direction at joint point N; and α_2 is the angle between tooth tip force F_V and the X-axis direction.

Furthermore, we have

$$F_{2Y}=F_{2X}\tan\alpha_5, \tag{17}$$

$$F_{QY}=F_{QX}\tan\alpha_3, \tag{18}$$

$$F_{NY}=F_{NX}\tan\alpha_4, \tag{19}$$

$$\alpha_2=\alpha_1-\angle QVX, \tag{20}$$

$$\alpha_3=\arctan\left(\frac{N_Y-Q_Y}{Q_X-N_X}\right), \tag{21}$$

$$\alpha_4=\arctan\left(\frac{M_X-N_X}{M_Y-N_Y}\right), \tag{22}$$

$$\alpha_5=\arctan\left(\frac{G_Y-M_Y}{M_X-G_X}\right), \tag{23}$$

where α_3 is the angle between the X-axis and connecting line of joint point N and joint point Q; α_4 is the angle between the Y-axis and the connecting line of joint point N and joint point M; and α_5 is the angle between the force F_2 and the Y-axis.

According to above equations, the relationship between the joint point force F_2 and the tooth tip tangential load F_V can be obtained.

3 Cross-section stress analysis of linkage mechanism under typical conditions

When the tooth tip of the bucket is subjected to digging resistance, the linkage mechanism is the most direct force transmission mechanism between the bucket cylinder and the bucket. The relationship between the hinge point force and the tooth tip load is used to further

analyze the variation of cross-section stress of linkage mechanism with the joint point force. Consequently, the relationship between the cross-section stress and the tooth tip's digging force is obtained.

Due to complex stress situation of the excavator's components, the subsequent simulation only considers the stress of the linkage structure under the action on the bucket of hydraulic cylinder.

3.1 Determination of location for stress measurement

Two points should be paid attention to when choosing the cross section for actual measurement. Firstly, the area where the changes in stress and strain are more obvious is selected as the measurement location. Secondly, the selected section should avoid the location where the welding point and joint point are connected to the working device. ANSYS software was used to apply a horizontal force of 28 kN to the bucket tooth tip and analyze the stress distribution of the intermediate linkage. The results are shown in Fig.3.

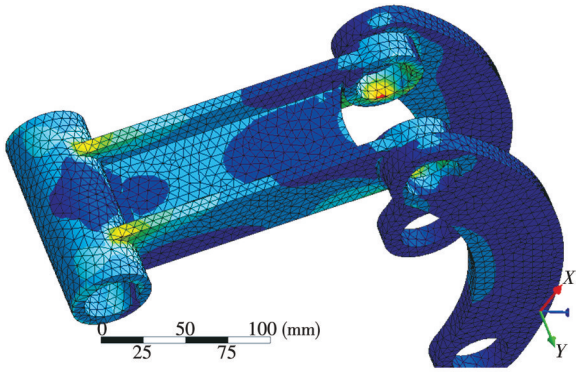

Fig. 3 Equivalent cross-section stress distribution cloud diagram of middle connecting rod

According to the stress analysis results of the connecting rod, it can be observed that the joint point connection of the parts and the connecting rod section at 0.08 m from the joint point have more obvious stress changes. However, considering the subsequent stress measurement requirements, it is difficult to ensure the arrangement of sensors at the joint point connection, so a distance of 0.08 m from the bucket joint point on the connecting rod is selected as the measurement section.

3.2 Calculation of cross-section stress

According to the analysis results of the applied load at each joint point of the bucket linkage mechanism above, the calculated component forces F_{2X} and F_{2Y} of joint point M are not the forces along the cross-section direction of the connecting rod, so it is necessary to change the load at joint point M that is decomposed along the cross-section direction of the linkage mechanism. Then, the decomposed load with the parameters of the measured location is used to obtain the normal stress of each measurement point. As shown in Fig.4, joint point M is taken as the origin of the coordinates to establish a local coordinate system, with the X_1-axis along the MK direction of the connecting rod and the direction from M to K as positive as well as the Y_1-axis perpendicular to the line MK and the outer direction of the bucket as positive. The load generated at joint point M can be expressed in this local coordinate system as

$$F_{X1} = F_2\cos(2\pi - \angle GMK), \tag{24}$$

$$F_{Y1} = F_2\sin(2\pi - \angle GMK), \tag{25}$$

$$\angle GMK = \angle GMN + \angle NMK. \tag{26}$$

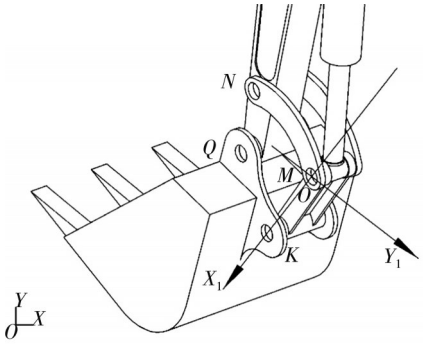

Fig. 4 Local coordinate system at hinge point *M*

Since the selected connecting rod section is an I-shaped cross-section, the normal stress on the cross-section is linearly distributed along the axial direction. The connecting rod section should be subjected to a normal force perpendicular to the connecting rod section and a concentrated force along the section direction. In the cross-section stress calculation, because the section has shear stress that belongs to plane stress, it should be calculated separately and it is not considered here. Based on the section parameters of the I-shaped section, the normal stresses generated by different loads at the selected section are calculated as

$$\sigma_{FX1} = \frac{F_{X1}}{A}, \tag{27}$$

$$\sigma_{FY1} = \frac{F_{Y1}Bl}{2I_Z}, \tag{28}$$

$$\delta_t = \sigma_{F_{X1}} + \sigma_{F_{Y1}}, \tag{29}$$

where A is the cross-section area of the connecting rod; B is the section height; l is the distance from the hinge point of the section to the measured section; I_Z is the moment of inertia of the cross-section around the Z-axis, σ_{FX1} is the normal tensile stress; σ_{FY1} is the normal bending stress; and δ_t is the cross-section stress.

The coordinates of point C are known in the

established global coordinate system of the working device. The dynamic coordinatees of the key hinge points can be obtained by substituting the coordinates of point C into Eqs. (1) — (8). Then, the relationship between F_2 and F_V can be derived from the established torque equation and force balancing equation of the bucket and linkage mechanism. Finally, according to the knowledge in material mechanics, the mathematical relationship between the stress of the measured section and the digging force is obtained. Assuming that the length of the hydraulic cylinder of the boom is 0.89 m, the length of the hydraulic cylinder of the bucket rod is 1 m, and the length of the hydraulic cylinder of the bucket is 0.8 m, the relationship curve between the cross-sectional stress of the linkage mechanism and the digging force can be obtained for the excavator in the determined location, and the error between simulation results and theoretical results is about 8%, as shown in Fig.5.

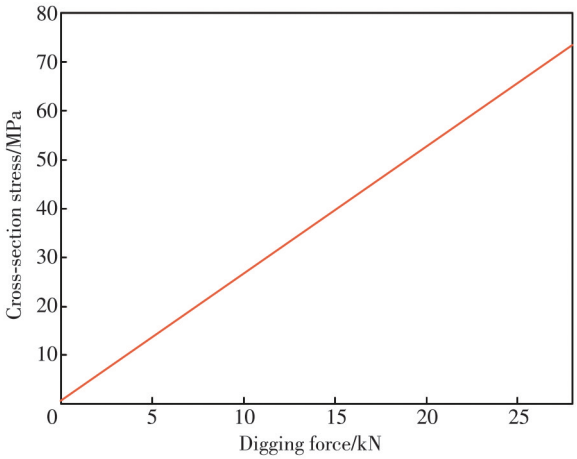

Fig. 5 Relationship curve between digging force of tooth tip and cross-section stress of connecting rod

4 Simulation

4.1 Establishment of three-dimensional finite element model

We used UG to establish a three-dimensional model of excavator arm, as shown in Fig. 6. An interface between UG and ANSYS Workbench was used for the seamless transfer of data, which avoids the loss of data and effectively compensates for the shortfalls of Workbench.

4.2 Definition of element type and material properties

The material of the excavator arm was set be Q345, and the material of other parts was set to be 42CrMo. The material properties are shown in Table 1. The bucket structure of hydraulic cylinder is similar to a stepped shaft. According to the selection requirements of the finite element unit, this study meshed with 3D 20-node structural SOILD186. The rest of the physical parts adopted the software default unit type. The hinge part adopted the contact analysis method, and it is considered that the two parts in contact are regarded as separate flexible bodies rather than rigid bodies, so as to simulate the deformation of the parts in motion and the changes of mutual forces and displacements[15-17].

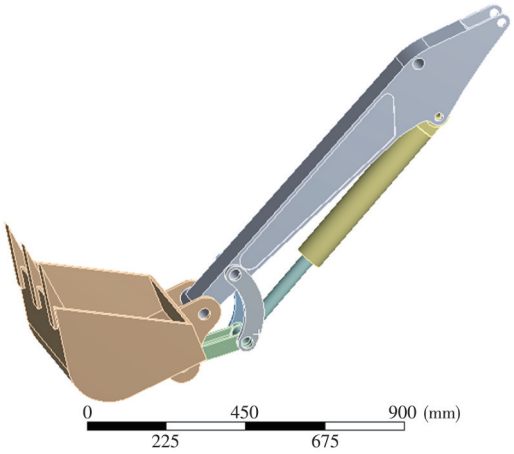

Fig. 6 Three-dimensional model of partial mechanism of excavator

Table 1 Material properties

Materials	Poisson's ratio	Elastic modulus/GPa	Density/(kg•m^{-3})	Yield strength/MPa	Shear modulus/GPa
Q345	0.280	206	7 850	345	79.00
42CrMo	0.280	212	7 850	930	79.38

4.3 Settings of boundary conditions and mesh division

According to Ref.[18], cylindrical support was applied to the hinge, which constrained the axial, radial and circumferential directions of the cylindrical hole; Applying displacement constraint on the hinge of the linkage mechanism constrained the displacement in the X-axis direction while released the displacement in the other two directions. For the joint point, the force boundary conditions were applied. Considering the stress distribution of the hinge hole, the cosine loading method was adopted while the gap between the pin shaft and the shaft hole was ignored. The mesh was divided by the patch conforming method under Tetrahedrons in the software, and the whole model was divided into 259 332 units and 413 730 nodes. The finite element model was established, as shown in Fig.7.

In the developed excavator model, the relationship between digging force and digging resistance results

from action and reaction forces[19]. Therefore, the digging force of the hydraulic cylinder on condition that the bucket rod was locked was applied uniformly to the model of the bucket teeth as digging resistance. To better compare with the theoretical values, the tooth tip load was applied from 10 kN to 28 kN, which is the theoretical maximum digging force that the selected excavator prototype can achieve.

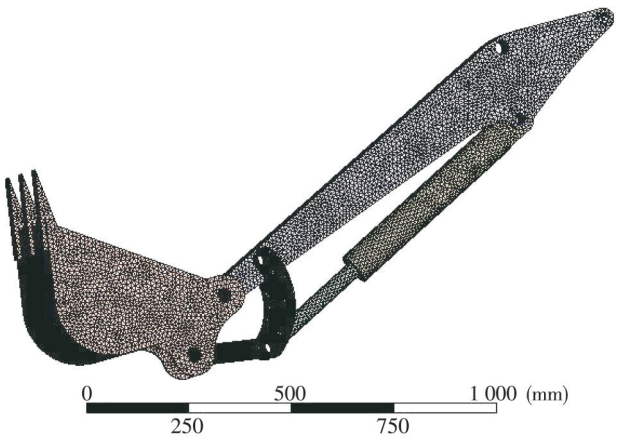

Fig. 7 Meshed model

4.4 Cross-section stress path of linkage mechanism

According to theoretical analysis, the mathematical relationship between the cross-section stress of linkage mechanism and the digging force was obtained. To better reflect the change of stress on the cross-section of the linkage mechanism, the stress path was set in the area at 0.08 m from the connection point between the bucket and the linkage mechanism, as shown in Fig. 8. The average stress on the path is the stress of the measured section of the connecting rod by simulation.

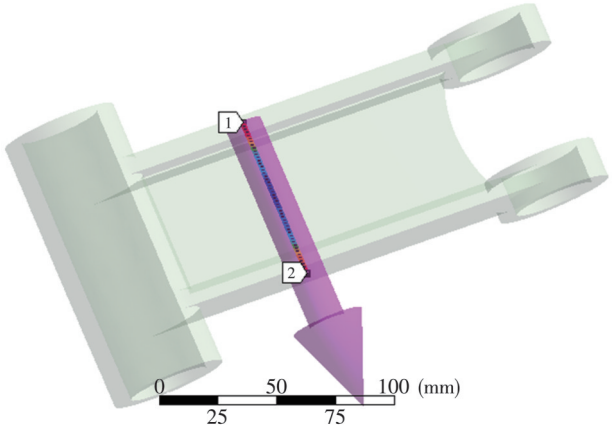

Fig. 8 Stress path of connecting rod

4.5 Results and discussion

Co-simulation using UG and ANSYS workbench was conducted, and the cross-section stress change of the connecting rod at 0.08 m under the change of tooth tip digging force (F) was obtained. The theoretical cross-section stress value was compared with that by the Workbench simulation, and the results are shown in Table 2, where σ_t is the theoretical value and σ_f is the simulation result.

Table 2 Cross-section stress and error of connecting rod by theoretical calculation and simulation

No.	F/kN	σ_t	σ_f	Error$\left(\frac{\sigma_t-\sigma_f}{\sigma_t}\right)$
1	10.0	28.166	30.296	0.075
2	11.5	32.337	34.840	0.077
3	13.0	36.509	39.385	0.078
4	14.5	40.680	43.928	0.079
5	16.0	44.851	48.468	0.080
6	17.5	49.023	53.006	0.081
7	19.0	53.194	57.543	0.081
8	20.5	57.366	62.078	0.082
9	22.0	61.537	66.613	0.082
10	23.5	65.708	71.148	0.082
11	25.0	69.880	75.683	0.083
12	26.5	74.051	80.217	0.083
13	28.0	78.222	84.749	0.083

According to the data shown in Table 2, a comparison curve between the theoretical and simulated stresses in the cross section of the linkage mechanism was drawn using Matlab, as shown in Fig. 9. It can be seen that the trend of the theoretical curve is consistent with that of the simulation curve, and the error is about 8%.

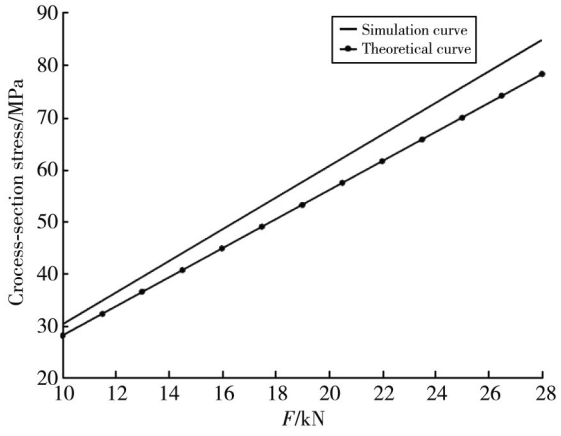

Fig. 9 Contrast curves of theoretical and simulation values of cross-section stress of connecting rod

5 Conclusions

In this study, we established the global coordinate system of the excavator's working device as well we its general mechanism model. In the global coordinate system, we analyzed the kinematic relationship between the major components of the excavator's and established a mathematical model for calculating the theoretical

digging force of the whole machine under typical working conditions Furthermore, we established the calculation model of the hinge force in the linkage mechanism. By analysis of the connecting rod structure, according to the parameters of section and the calculation model of hinge force, we obtainded the coupling relationship between the cross-section stress of connecting rod and the digging force as well as the mathematical model for measuring "connecting rod stress-digging force". Finally, we used three-dimensional software and finite element analysis software to co-simulate the working devices of the excavator, and then compared the simulated stress change value with the theoretical calculation value. The results show that the digging force measuring model proposed is feasible.

Acknowledgement

This work was supported by Key Project of Industrial Science and Technology of Shaanxi Province (No.2015 GGY068)

Declaration of conflicting interests

The authors have no conflict of interests related to this publication.

References

[1] LI Y H, FAN R J, YANG L M, et al. Research status and development trend of intelligent excavators. Chinese Journal of Mechanical Engineering, 2020, 56(13): 165-178.

[2] WEN S H. Design of remote control and monitoring system for electric excavators based on wireless communication. Quanzhou: Huaqiao University, 2020.

[3] CAI Z Y, WANG Z K, CHEN T H, et al. Real-time detection method for excavators from the perspective of drones based on YOLOv3. Journal of Ningbo University (Science and Technology Edition), 2021, 34(2): 42-48.

[4] SUN W, LI E Y, WANG X B, et al. Optimal mining trajectory planning for intelligent excavators. Journal of Dalian University of Technology, 2018, 58(3): 246-253.

[5] JIANG P, LU X M, WANG T, et al. Hydraulic system of new hydraulic excavator based on load independent flow distribution system. Opencast Mining Technology, 2021, 36(1): 55-57.

[6] REN Z G, WANG J L, ZOU Z H, et al. Modeling of the Limiting digging force of hydraulic excavator based on resistance characteristics. Mechanika, 2019, 25(5): 357-362.

[7] FLORES F G, KECSKEMÉTHY A, POTTKER A. Workspace analysis and maximal force calculation of a face-shovel excavator using Kinematical transformers//12th IFToMM World Congress on Mechanism and Machine Science, June 18-21, 2007, Besancon, France. Berlin: Springer, 2007: 2906-2911.

[8] BAI Y P. Simulation analysis and research on digging force of hydraulic excavator. Journal of Taiyuan University of Science and Technology, 2021, 42(1): 54-58.

[9] JIANG W L, ZHANG S Q, LI J T, et al. Development of sensors for indirect measurement of excavation resistance. Journal of Yanshan University, 1998(2): 42-44.

[10] YU L P, LU Y, XIANG Y S, et al. Test method of bucket load of hydraulic excavator. Chinese Journal of Engineering Machinery, 2016, 14(3): 267-270.

[11] CHEN Q G, GUO C, HU P, et al. Measuring method of excavation resistance based on pin sensor. Journal of Beijing University of Technology, 2017, 43(8): 1135-1140.

[12] TAO S, HAO G, LIU G Z, et al. Measurement method for maximum digging force of backhoe bucket cylinder. Mechanical Engineer, 2014(8): 45-47.

[13] JI M Z. Programmatic drawing of excavation performance graph of hydraulic excavator backhoe device based on Matlab. Chongqing: Chongqing University, 2006.

[14] LI G Y. Force analysis and finite element simulation of hydraulic excavator bucket cylinder. Architectural Engineering Technology and Design, 2016(10): 2378-2379.

[15] LANAKIEV A, DONEV K. Investigation into dynamic analysis of complex structures using superelements// Simulation in Industry January 1, 1996, Genoa, Italy. 1996: 212-216.

[16] ZHOU H B, WANG H K, GUO X H, et al. Static strength analysis of excavator working device structure based on MATLAB and ANSYS. Journal of Guangxi University (Natural Science Edition), 2009, 34(6): 5-6.

[17] PANG C L, WANG X Q, WANG W C, et al. Optimization and improvement of excavator stick structure based on finite element analysis. Construction Machinery Technology and Management, 2021, 34(2): 72-73.

[18] SU Q, ZHAO H Q, WANG K, et al. Simulation analysis of static strength of excavator working device. Computer Simulation, 2014, 31(11): 198-202.

[19] WANG X J, SUN H R, FENG M H, et al. Dynamic analysis of working device of excavator under limit digging force. Journal of the Institution of Engineers, Series C, 2021, 102(5): 1137-1144.

液压挖掘机齿尖挖掘力的间接检测方法

孙天宇*, 张　平, 张　森, 佟昆宏

西安建筑科技大学 机电工程学院, 陕西 西安 710055

摘　要： 液压挖掘机的挖掘力是反映挖掘机工作状态的一个重要参数。基于挖掘机工作装置的力学分析, 建立了反应连杆机构截面应力与铲斗挖掘力之间关系的数学模型, 并提出了一种新的挖掘力测量方法。通过有限元模拟分析, 得到了连杆机构截面应力在不同挖掘力的仿真结果, 与理论计算的误差约为8%。仿真结果验证了该测量方法的可行性。

关键词： 液压挖掘机; 应力检测; 挖掘力; 有限元仿真

引用格式： SUN Tianyu, ZHANG Ping, ZHANG Sen, et al. Indirect measurement method for digging force of hydraulic excavator. Journal of Measurement Science and Instrumentation, 2024, 15(1): 1-8.